fractal and fractional

Article

Effect of Heterogeneity on the Extension of Ubiquitiformal Cracks in Rock Materials

Beibei Yang, Xiaoshan Cao *, Tielin Han, Panfeng Li and Junping Shi

Department of Mechanics, School of Civil Engineering and Architecture, Xi'an University of Technology, Xi'an 710048, China; 1200713012@stu.xaut.edu.cn (B.Y.); s3050210133@163.com (T.H.); 2200721121@stu.xaut.edu.cn (P.L.); shijp@xaut.edu.cn (J.S.)

* Correspondence: caoxsh@xaut.edu.cn

Abstract: Fracture energy, as an important characteristic parameter of the fracture properties of materials, has been extensively studied by scholars. However, less research has been carried out on ubiquitiformal fracture energy and the main method used by scholars is the uniaxial tensile test. In this paper, based on previous research, the first Brazilian splitting test was used to study the ubiquitiformal crack extension of slate and granite, and the complexity and ubiquitiformal fracture energy of rock material were obtained. The heterogeneity of the material was then characterized by the Weibull statistical distribution, and the cohesive model is applied to the ABAQUS numerical software to simulate the effect of heterogeneity on the characteristics of ubiquitiformal cracks. The results demonstrate that the ubiquitiformal complexity of slate ranges from 1.54 to 1.60, and that of granite ranges from 1.58 to 1.62. The mean squared deviations of the slate and granite ubiquitiformal fracture energy are the smallest compared with the other fracture energies, which are 0.038 and 0.037, respectively. When the homogeneity of the heterogeneous model is less than 1.5, its heterogeneity has a greater influence on the Brazilian splitting strength, and the heterogeneity of the rock is obvious. However, when the homogeneity is greater than five, the effect on the Brazilian splitting strength is much less, and the Brazilian splitting strength tends to be the average strength. Therefore, it is particularly important to study the fracture problem of cracks from the nature of the material structure by combining the macroscopic and mesoscopic views through the ubiquitiform theory.

Keywords: ubiquitiformal fracture energy; ubiquitiformal complexity; heterogeneity; homogeneity; Brazilian splitting strength

Citation: Yang, B.; Cao, X.; Han, T.; Li, P.; Shi, J. Effect of Heterogeneity on the Extension of Ubiquitiformal Cracks in Rock Materials. *Fractal Fract.* **2022**, *6*, 317. https://doi.org/10.3390/fractalfract6060317

Academic Editors: Xin Cai, Xiaohan Yang and Lihai Tan

Received: 11 May 2022

Accepted: 31 May 2022

Published: 5 June 2022

1. Introduction

Fractal geometry provides an important theoretical basis for the study of complex nonlinear problems. Manderlbrot et al. [1] first discovered that the fracture surface of steel had fractal characteristics, and since then the fractal characteristics of other material sections were confirmed [2–5]. Thus, fractal fracture mechanics provide a good method for the study of the fracture of rock-like materials that present irregularities and complexity. The research on fractals began with experimental studies on the fractal characteristics of sections [6–9] and then went on to study the relationship between fractal dimension and macroscopic fracture parameters [10–13]. Nowadays, with the help of numerical simulation software, fractal fracture models for different materials have been established to simulate the crack extension process in various material sections [14–18].

However, the inability to establish the edge value problem of fractal crack extension and the essential difficulty that the integer dimensional measure of fractal crack is singularity or divergence are faced in fractal applications. These challenges seriously hinder the development of fractal fracture mechanics research. To avoid this intrinsic difficulty in fractal applications, Ou et al. [19] proposed the concept of ubiquitiform based on fractal theory. The theory holds that the geometry of nature is ubiquitiform geometry rather than fractal geometry and that geometric or physical objects in nature are more reasonably described by ubiquitiform. Given that ubiquitiform theory is derived from fractal theory, they are closely related in mathematical formulation and have many commonalities. The difference between them is mainly reflected in the definition and processing of measures and dimensions. The introduction of a lower bound on the metric scale in the ubiquitiform makes the measure finite, thereby allowing the ubiquitiform to be applied to the characterization of practical problems better. In terms of dimensionality, the ubiquitiform is generated from an integer-dimensional initial structure by a finite number of self-similar iterations [20]. Thus, it has an integer number of dimensions, which avoids the trouble caused by the dimension change in the gauge problem. Currently, due to the advantages of ubiquitiform geometry in the description of complex fine structures, it has been well used in recent years. Li et al. [20] used the ubiquitiform geometry to describe the concrete crack development process and obtained the ubiquitiformal fracture energy of concrete. Ou et al. [21] analyzed the size effect of fracture energy on the basis of Li's study. Li et al. [22] found that the strain rate had an effect on the extension path of ubiquitiformal fracture. Looking at the previous research work, it is not difficult to find that since the application of the ubiquitiform theory to the study of fracture problems. The conclusions obtained are more realistic than the results calculated by conventional fracture theory. The cracks formed under the action of load in the actual working condition are of self-similar characteristics. Then, this self-similarity feature cannot be neglected in the calculation of the crack problem. Therefore, based on the previous research, Zhang [23] investigated the crack extension of different crack specimens under load based on the analytical method of ubiquitiform theory. The results were obtained in better agreement with the engineering reality.

The extension path of the cracks under Brazilian splitting action shows a more obvious ubiquitiformal feature. This feature is also a reflection of the random non-uniform distribution of materials within the rock. The Weibull statistical distribution is widely used to reflect the heterogeneity of rock materials. You and Zou [24] discussed the effect of heterogeneity and size of rock materials on the strength of specimens. In recent years, with the rapid development of computer technology, more scholars have adopted numerical methods to study heterogeneous materials [25–27]. The heterogeneity of rocks in numerical simulations can be characterized in two ways. The first one is the heterogeneity of rock mechanical parameters, such as the mechanical parameters of rock units obeying Weibull distribution in RFPA software [28,29]. The results showed that the heterogeneity had a great influence on the strength and crack extension of the specimens under compression loading. The second one is the heterogeneity of the mesostructure of the rock. For example, Lan et al. [30] investigated the effect of heterogeneity of the mesostructure on the model stress distribution and crack extension problems by using UDEC software. On the other hand, tensile strength is very important in rock damage analysis because it is much lower than compressive strength and triggers tensile damage more easily. For example, in the Brazilian splitting test, the stress distribution of a homogeneous specimen is uniform, while for a heterogeneous specimen, the stress field is intricate. Liao et al. [31] used numerical simulations to investigate and explain the differences in rock tensile strength between the direct tensile test, the Brazilian splitting test, and the three-point bending test. Thus, the tensile crack behavior will vary with heterogeneity.

Usually, the crack surface has a very irregular structure, which macroscopically looks similar to a chaotic structure and exhibits a complex phenomenon of bending irregularities. However, observations at a certain microscopic scale have statistical self-similar properties. Numerous experiments have shown that these fracture surfaces, or cracks, have a ubiquitiformal feature [20,32,33]. For this reason, this paper relates the fracture parameter, a macroscopic mechanical quantity, to the ubiquitiformal feature of the material's cross-sectional structure. As such, a ubiquitiformal fracture energy that balances the need for microscopic fracture characteristics and macroscopic fracture mechanics analysis is proposed. Furthermore, the Weibull statistical distribution is used to represent the heterogeneity of the material, and the effect of heterogeneity on the ubiquitiformal crack characteristics is studied by numerical method.

2. Brazilian Splitting Test of Slate and Granite Specimens

2.1. Test Equipment and Specimen Preparation

Slate and granite were selected as the research objects of this paper. The slate has an obvious plate structure and is mostly dark gray to light gray in appearance. Granite is the product of magmatic activity and is an igneous rock. During the processing of the specimen, a cylindrical specimen with a diameter of 50 mm and a height of 100 mm was first drilled using the dry drilling method. Subsequently, the specimen was machined into a cylinder with a diameter of 50 mm and a thickness of 25 mm according to ISRM standards. Six of each type of rock were used as a group, a total of two groups. One group was selected for the Brazilian splitting test, and the other group was used for the uniaxial compression test (Table 1). The equipment used in the Brazilian splitting and uniaxial compression tests in this paper is the WDT-1500 multi-functional material testing machine [34]. The rock specimens were loaded using displacement control with loading rates of 0.5 mm/min (Figures 1 and 2).

Table 1. Test data and calculation results of slate specimens.

Specimen	f_t (MPa)	E (GPa)	δ_{min} (μm)	D	G (N/mm)	K_{IC} (MPa·mm$^{1/2}$)	G_c (N/mm)	G_{uf} (N/mm)
S-1	4.929	9.858	1.4	1.55	0.6661	0.1115	0.1261	0.2086
S-2	7.140	10.710		1.60	1.1893	0.1615	0.2437	0.2206
S-3	6.085	9.128		1.56	0.9549	0.1377	0.2077	0.2693
S-4	4.652	9.304		1.57	0.7861	0.1053	0.1190	0.2277
S-5	5.432	10.864		1.58	0.9993	0.1229	0.1390	0.2524
S-6	5.116	8.185		1.54	0.7049	0.1157	0.1800	0.3080

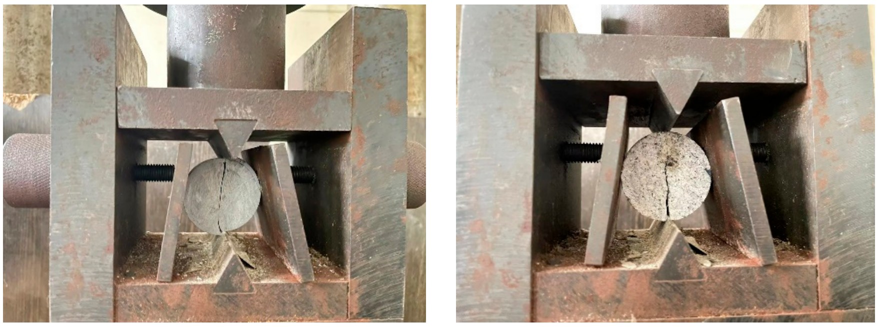

(**a**) Slate (**b**) Granite

Figure 1. Brazilian splitting test.

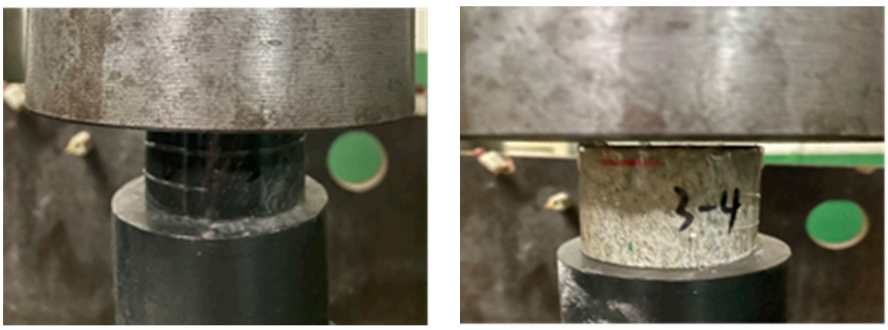

(**a**) Slate (**b**) Granite

Figure 2. Uniaxial compression test.

2.2. Calculation of the Ubiquitiformal Complexity of Slate and Granite Specimen Sections

Ubiquitiform theory holds that the geometry of nature is ubiquitiform geometry rather than fractal geometry and that geometric or physical objects in nature are more reasonably described by ubiquitiform. Considering that ubiquitiform theory is derived from fractal theory, they are closely related in mathematical formulation and have many commonalities. The difference between them is mainly reflected in the definition and processing of measures and dimensions. The introduction of a lower bound on the metric scale in the ubiquitiform makes the measure finite, which allows the ubiquitiform to be applied better to the characterization of practical problems [35]. Currently, due to the advantages of ubiquitiform geometry in describing complex fine structures, it has been used well in the field of rock mechanics in recent years [22].

In ubiquitiform geometry, ubiquitiformal complexity is used to measure the unevenness of the curve. The ubiquitiformal complexity can be measured in many ways, the most common of which is the box-counting method. In this paper, the damaged slate and granite specimens were obtained by Brazilian splitting tests (Figure 3). Then, it relies on digital image analysis and the calculation of the box dimension algorithm based on MATLAB. The relationship curve between the measurement and the scale invariance in double logarithmic coordinates is obtained and fitted, and the slope is the complexity of the ubiquitiform curve. That is,

$$D = -\frac{\lg N(\delta)}{\lg \delta} \tag{1}$$

where $N(\delta)$ is the number of boxes, and δ is the changing box size.

Figure 3. Failure patterns of some specimens under static load (slate and granite).

Figure 4 shows the box-counting method double logarithmic diagram for slate and granite. The slope (complexity) of the slate specimens does not differ greatly. Similarly, the slope of the granite specimens fluctuates in a small range, but the slope of the granite is generally larger than that of the slate (Tables 1 and 2). The slate is a metamorphic rock with an obvious plate structure and often appears as a flat fracture surface after being stressed. Granite is an igneous rock with complex chemical composition, and the main mineral components are quartz, orthoclase, and biotite. These minerals are very unevenly distributed. As a result, the cracks are rougher, and the complexity is greater compared with that of slate.

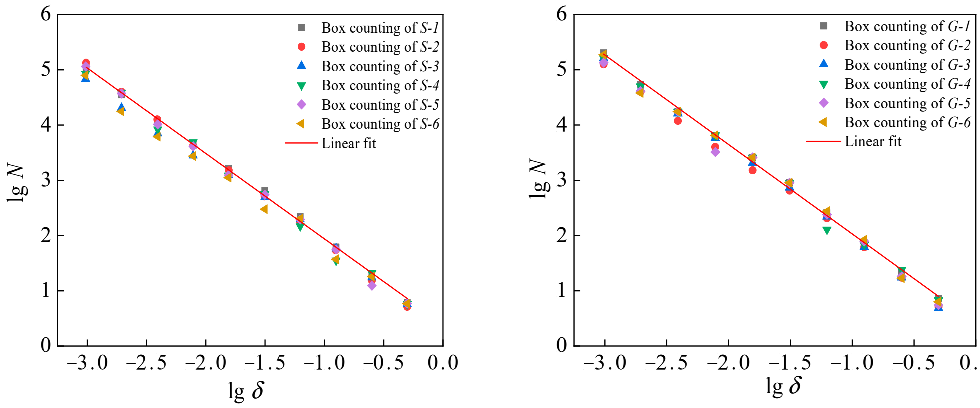

Figure 4. Box-counting method double logarithmic diagram for slate and granite.

Table 2. Test data and calculation results of granite specimens.

Specimen	f_t (MPa)	E (GPa)	δ_{min} (μm)	D	G (N/mm)	K_{IC} (MPa·mm$^{1/2}$)	G_c (N/mm)	G_{uf} (N/mm)
G-1	10.519	15.779	4.7	1.61	2.6287	0.2380	0.3590	0.2744
G-2	8.553	13.685		1.58	2.2706	0.1935	0.2736	0.3448
G-3	9.792	14.687		1.62	2.5781	0.2215	0.3342	0.2375
G-4	9.238	14.781		1.61	2.8987	0.2090	0.3956	0.3026
G-5	8.319	13.310		1.60	2.5606	0.1882	0.2662	0.3029
G-6	7.989	13.583		1.61	2.5081	0.1807	0.2406	0.2618

2.3. Ubiquitiformal Fracture Energy versus Conventional Fracture Energy

To investigate the fracture problem of rocks under ubiquitiform theory, the ubiquitiform characteristics of crack extension paths in brittle materials are considered in this paper. Based on the Griffith energy principle, the complexity and the lower bound to scale invariance are introduced into the expression of fracture parameters. The derivation process is presented as follows.

First, in this paper, the damage behavior of rocks under Brazilian splitting conditions is studied, and the tensile strength of rocks can be calculated from Brazilian splitting,

$$\sigma = \frac{2P}{\pi Dt} \tag{2}$$

where σ is the Brazilian splitting strength; P is the maximum load; and D and t are the diameter and thickness of the rock disc, respectively.

Second, the cracks of slate and granite during Brazilian splitting damage are type I cracks, in which the energy required to form a unit area crack is defined as the fracture energy. In classical fracture mechanics, the fracture energy can be expressed as,

$$G = \frac{W}{A} = \frac{W}{R \cdot t} \tag{3}$$

where W is the work performed by the load, A is the cross-sectional area of the smooth section, R is the diameter of the specimen, and t is the thickness of the specimen.

However, the fracture energy in classical fracture mechanics only considers the cross-sectional area of a smooth section, whereas type I cracks are actually rough. Therefore, considering its true crack extension path is necessary. Rock materials were confirmed to have ubiquitiform features [36]. When the material cross-section is described as a ubiquitiform, its actual cross-sectional area is different from the smooth cross-sectional area, thereby resulting in a corresponding change in fracture energy. Under ubiquitiform theory, when considering the ubiquitiform features in the thickness direction, the fracture energy can be expressed as,

$$G_{uf} = \frac{W}{A_{uf}} = \frac{W}{R^D \cdot t^D \cdot \delta_{\min}^{2-D}} \tag{4}$$

where W is the work performed by the load, A_{uf} is the ubiquitiformal cross-sectional area, δ_{min} is the lower bound to scale invariance, and D is the ubiquitiformal complexity. Simultaneous Equations (3) and (4) can be obtained,

$$\frac{G_{uf}}{G} = \frac{(R \cdot t)^{1-D}}{\delta_{\min}^{2-D}} \tag{5}$$

However, for rock materials, the fracture energy can also be obtained from the fracture toughness and elastic modulus under the assumption of linear elasticity, as shown in Equation (6),

$$G_c = \frac{K_{IC}^2}{E} \tag{6}$$

Wang et al. [37] proposed to determine the fracture toughness by the minimum local load $\sigma_{\min}$ after the central initiating load. For the specific loading angle in this paper, the fracture toughness is expressed as,

$$K_{IC} = 0.80\frac{\sigma_{\min}}{\sqrt{Rt}} \quad \left(2\alpha = 20^\circ\right) \tag{7}$$

Finally, according to Equation (3), the corresponding fracture energy of the smooth section of the slate and granite specimens can be found. The fracture energy of the rock material is also obtained from the relationship between the fracture energy and the fracture toughness in Equation (6) and its ubiquitiformal fracture energy in Equation (5). By comparison, the ubiquitiformal fracture energy is closer to the fracture energy obtained by the relationship between fracture energy and fracture toughness, as shown in Tables 1 and 2.

According to Tables 1 and 2, the elastic modulus of slate varies in the range of 8.19–10.86 GPa, and the elastic modulus of granite varies in the range of 13.31–15.78 GPa. The traditional fracture energy of slate and granite tends to increase with the elastic modulus. However, the ubiquitiformal fracture energy and the fracture energy calculated from the fracture toughness fluctuate in a certain range. This phenomenon is due to the fact that the same rock material has a good crack consistency when a fracture occurs. Therefore, the fracture energy does not differ greatly. In addition, although differences are observed in the elastic modulus of slate and granite, the difference in ubiquitiformal fracture energy is not significant.

The relationship between the fractal dimension of the material section and its fracture mechanical property parameters was provided by many scholars for different types of materials based on experimental results [38]. As shown in Figure 5, complexity is positively correlated with fracture energy. This conclusion is also consistent with those obtained from previous experiments [39]. The same rock material has a good crack consistency when a fracture occurs. Therefore, the fracture energy does not differ much. In this paper, the mean values and mean squared deviations of the three fracture energies for slate and granite were obtained, and the mean squared deviations of the ubiquitiformal fracture energy were the smallest compared with the other fracture energies. The mean squared deviations of slate and granite are 0.038 and 0.037, respectively, and the reliability of the ubiquitiformal fracture energy was further verified. In addition, the calculated results for the ubiquitiformal fracture energy G_{uf} are very close to the critical strain energy release rate G_c obtained from the fracture toughness relationship while differing significantly from the traditional fracture energy G. Therefore, the ubiquitiformal fracture energy is more consistent with the assumption of linear elastic fracture of brittle materials than the fracture energy measured under the assumption of the smooth fracture surface. A comparison of the ubiquitiformal complexity of slate and granite reveals that the ubiquitiformal complexity of slate specimens ranges from 1.54 to 1.60, and that of granite specimens ranges from 1.58 to 1.62. The ubiquitiformal complexity of the rock specimens clearly shows that the mechanical properties of rock materials are different because of the influence of heterogeneity. Therefore, investigating the effect of the heterogeneous properties of rock materials under Brazilian splitting conditions is necessary.

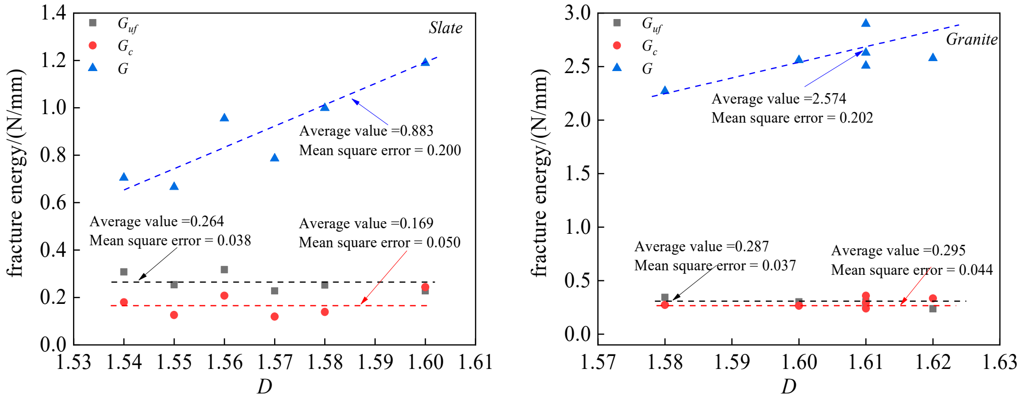

Figure 5. Three fracture energies and complexity D of slate and granite.

3. Numerical Simulation of Brazilian Splitting

In Section 2, we found that the extension path of cracks in the rock material during Brazilian splitting shows a ubiquitiformal feature. This ubiquitiformal feature reflects the heterogeneity of the internal mechanical properties of the material. Therefore, the Weibull distribution density function is used in this paper to describe the heterogeneity of the material and combined with ABAQUS numerical software to simulate the extension process of Brazilian splitting cracks. The numerical models in this paper are divided into two types of ideal homogeneous and heterogeneous models.

3.1. Cohesion Model

The cohesive model is a damage mechanics model that uses the traction-separation rule to simulate the decohesion of atomic lattice [40]. The cohesive model is a triangular model (Figure 6). di, df, and G_{IC} denote the initial damage displacement, effective displacement of traction force, and energy release rate, respectively. The model can simulate delamination failure and also random crack extension by batch inserting cohesive elements between adjacent solid elements in the model. When the contact traction or separation reaches the peak point T in Figure 6, the damage begins, and the cohesive element starts to damage [41]. The damage initiation criterion used in this paper can be written as,

$$p = \max\left\{ \frac{\sigma_n}{\sigma_n^0}, \frac{\tau_s}{\tau_s^0}, \frac{\tau_t}{\tau_t^0} \right\} \tag{8}$$

where σ_n is the normal traction force in the section, τ_s and τ_t are the two tangential traction forces in the section. σ_n^0, $\tau_s^0 \tau_t^0$ are the peak values of the anisotropic nominal stress. When p = 1.0, the damage starts.

After the peak point T, the cohesive stiffness starts to degrade. The stress of the damaged cohesive element can be expressed as,

$$\begin{aligned} &\sigma_n = \begin{cases} (1-C)\overline{\sigma_n}, & \overline{\sigma_n} \geq 0 \\ \overline{\sigma_n}, & otherwise \end{cases} \\ &\tau_s = (1-C)\overline{\tau_s} \\ &\tau_t = (1-C)\overline{\tau_t} \end{aligned} \tag{9}$$

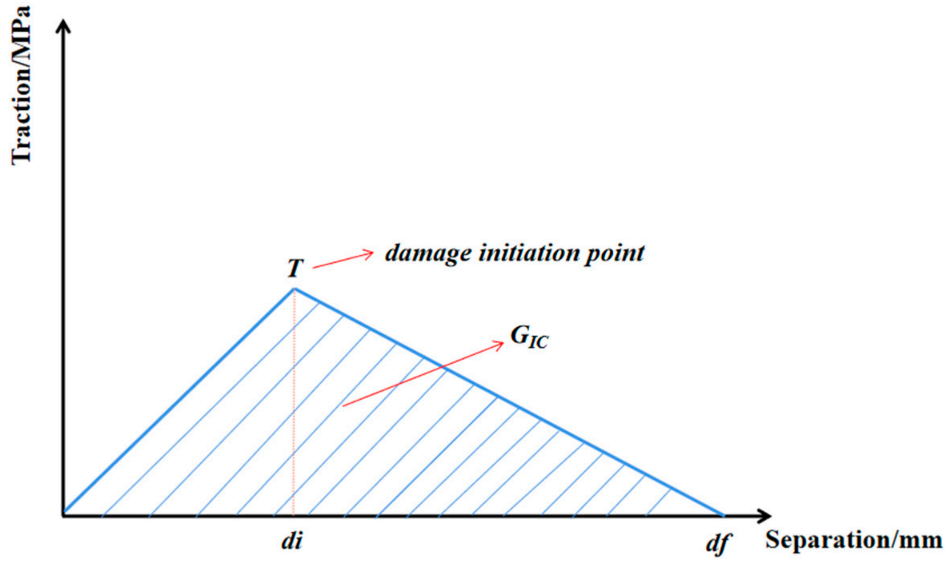

Figure 6. Cohesion model used in this paper.

C is the degree of damage. After the damage begins, C changes from 0 to 1. $\overline{\sigma_n}$, $\overline{\tau_s}$ and $\overline{\tau_t}$ are the contact stress components when no damage occurs, representing the overall damage of the contact point.

The model used in this paper is a plane strain model, as shown in Figure 7. The use of cohesive elements to simulate failure behavior in Brazilian splitting is an effective method. In the numerical model, the rock particles were represented by C3D8R elements with an edge length of 0.1 mm. In the C3D8R element, the cohesion element COH3D8 was embedded (Figure 8). The material parameters of the cohesion element were different from the rock material parameters. In addition, the thickness of all cohesive elements (COH3D8) was 1 mm.

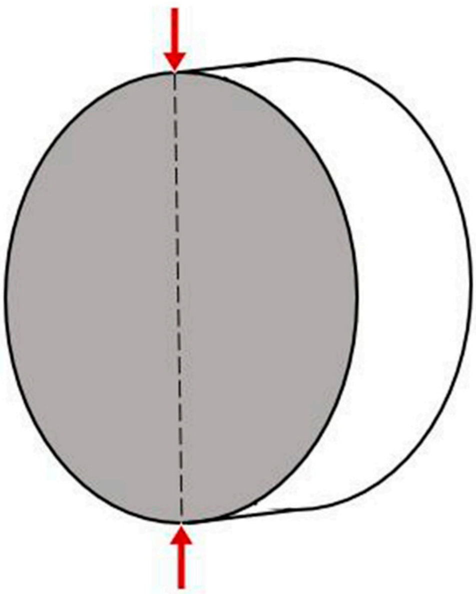

Figure 7. Finite element calculation model.

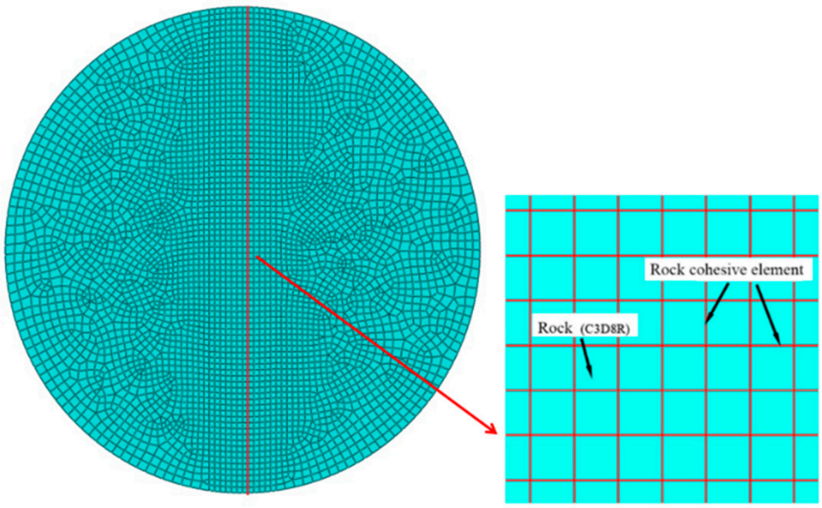

Figure 8. Finite element mesh.

3.2. Weibull Distribution of Elastic Modulus of Rock Materials

The rock is a typically brittle material and its internal material heterogeneity gives it a more rough and curved shape under Brazilian splitting conditions. As the elastic modulus is one of the most important parameters for representing the mechanical properties of materials, it is assumed that the elastic modulus of rock materials obeys the Weibull distribution as a random variable in this paper. In this paper, the steps to realize the finite element model of random heterogeneous materials satisfying the Weibull distribution are as follows. First, random samples are generated that satisfy the Weibull distribution, so that the random samples generated are different each time. However, they all obey the same Weibull distribution in a statistical sense, and their scale and shape parameters are the same. Next, the random sample data are mapped to a finite element model. The mapping approach taken in this paper is a one-to-one assignment of data and units, i.e., each random data corresponds to a unit. The Weibull distribution of the elastic modulus of the rock material is shown in Figure 9.

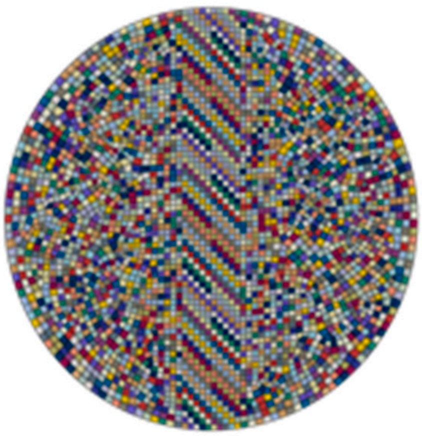

Figure 9. Weibull distribution.

3.3. Establishment of Numerical Model

In this paper, the cohesive model is applied to ABAQUS numerical software to simulate the failure behavior of rocks and to establish a simplified model of two-dimensional Brazilian splitting. This model is a plane strain model with a diameter of 50 mm and a thickness of 25 mm (Figure 7). The numerical test is described as follows: (1) The model mesh uses hexahedral elements and encrypts the area around 5 mm of the compressed diameter, and the whole model contains 4322 elements in total. The cohesive unit COH3D8 is embedded in these units with a unit thickness of 1 mm, as shown in Figure 8. (2) The analysis type is dynamic and explicit, with the upper and lower rigid bodies in surface-to-surface contact with the rock matrix and the contact friction coefficient set at 0.05. (3) A displacement load is applied at the top and a fully fixed boundary condition at the bottom with a loading rate of 0.001 mm per step. When the cohesive unit fails completely, SDEG = 1, the cohesive unit can no longer bear the force and will be deleted. The granite material parameters are shown in Table 3.

Table 3. Material properties of the numerical model.

***E*/GPa**	***μ***	***T*/MPa**	***di*/mm**	***df*/mm**	***GIC*/(N/mm)**
20	0.3	10.52	0.015	0.3	1.578

3.4. Results

3.4.1. Ideal Homogeneous Model

Figure 10 shows the ideal homogeneous model, and the simulation results are basically consistent with the experimental results. Under compressive loading, stress concentration occurs at the crack tip, and the stress is symmetrical about the crack plane. The damage begins when the stress at the crack tip reaches its maximum, and the crack develops along the central loading line until the material fails completely. The stress–displacement curves of the experimental and simulated values under this model are shown in Figure 11. The results show that the simulation results are in good agreement with the laboratory measurements, with the stress peaking at 0.3 mm and failing instantaneously. Figure 12 shows the box-counting method double logarithmic diagram for granite and the simulation results in a ubiquitiformal complexity of 1.65. The average ubiquitiformal complexity of the granite obtained from the test is 1.60 (Table 2), and the relative error between the two is 0.03%, which is in good agreement. This model is considered reasonable in simulating crack extension.

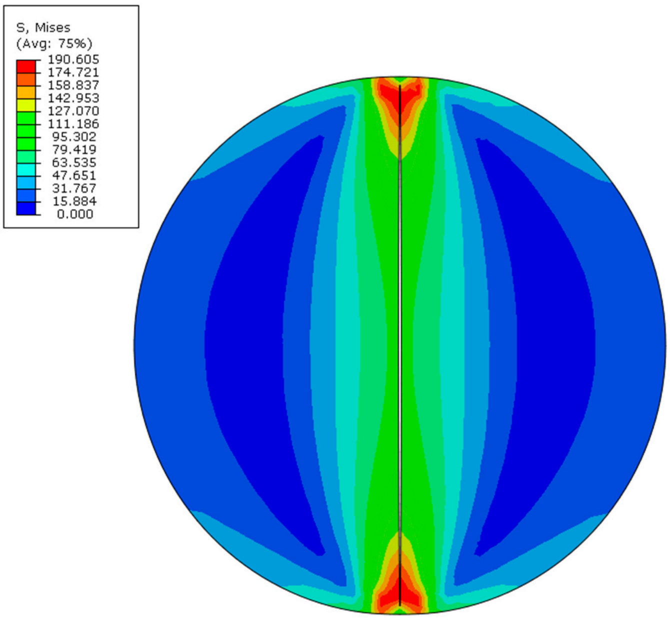

Figure 10. Numerical simulation of Brazilian splitting for ideal homogeneous model.

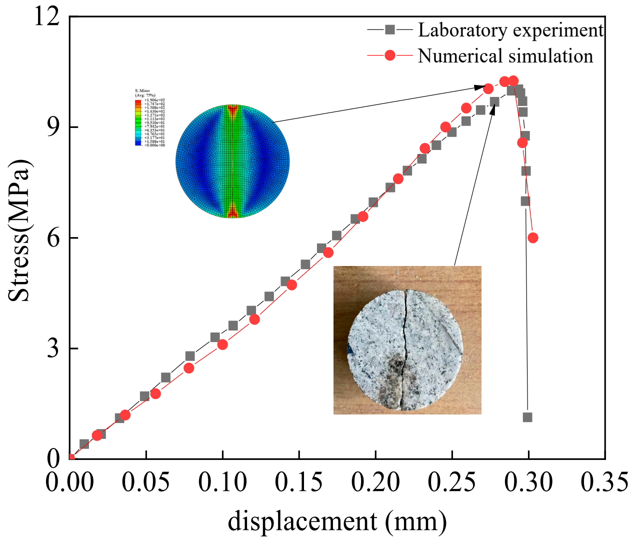

Figure 11. Comparisons of the stress–displacement curves measured in numerical simulation and laboratory experiments.

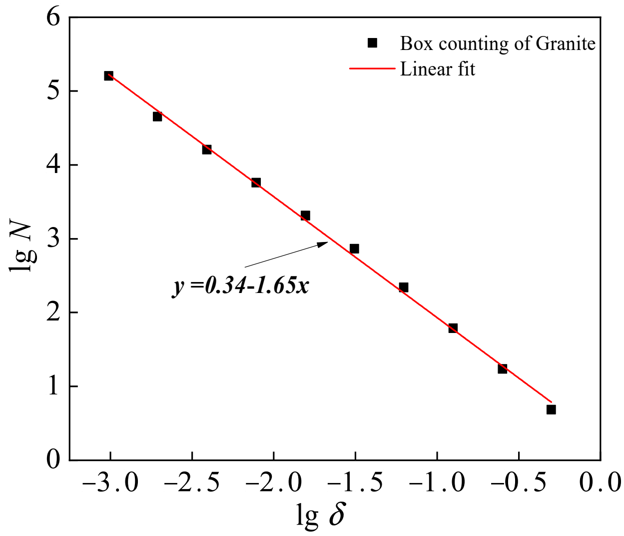

Figure 12. Box-counting method double logarithmic diagram for granite.

3.4.2. Heterogeneous Model

In nature, rocks are heterogeneous, and this heterogeneity is reflected in the fact that the mechanical properties of the material (e.g., elastic modulus, strength) vary with spatial location, hence violating the assumptions of the Brazilian test [42]. Therefore, heterogeneous properties may affect the accuracy of the determination of rock tensile strength using Equation (2). To study the effect of this property on the Brazilian strength, the elastic modulus of the mesoscopic element of the constituent material is assumed to satisfy the Weibull distribution. The Weibull distribution parameters m are set to 1.5, 5, 10, 100, and 1000.

As shown in Figures 13 and 14, for the numerical model with $m = 1.5$, the distribution of the stress concentration area is neither regular nor clear because of the discrete elastic modulus of the unit and the significant difference in stresses in adjacent units. The unit strength near the crack tip is also discrete, and the overall strength of the crack tip region is low. Thus, the stress concentration is at a low level. As the homogeneity increases (1.5–5), the discreteness of the unit strength and elastic modulus decreases, and the overall strength of the crack tip region increases and gradually converges to a constant. As a result, the stress is concentrated on a more regular and sharper profile. When the homogeneity is 1000, the mechanical properties improve rapidly. In addition, the Brazilian splitting strength decreases as the ubiquitiformal complexity increases. The heterogeneity of the rocks is evident at m of 1.5, and when $5 < m < 100$, the variation of the ubiquitiformal complexity of the rock is small, which belongs to low homogeneity. When m is 1000, the effect of the heterogeneous properties of the material is eliminated, which is reflected by the fact that the ubiquitiformal complexity is similar to that of m 5,10, and 100.

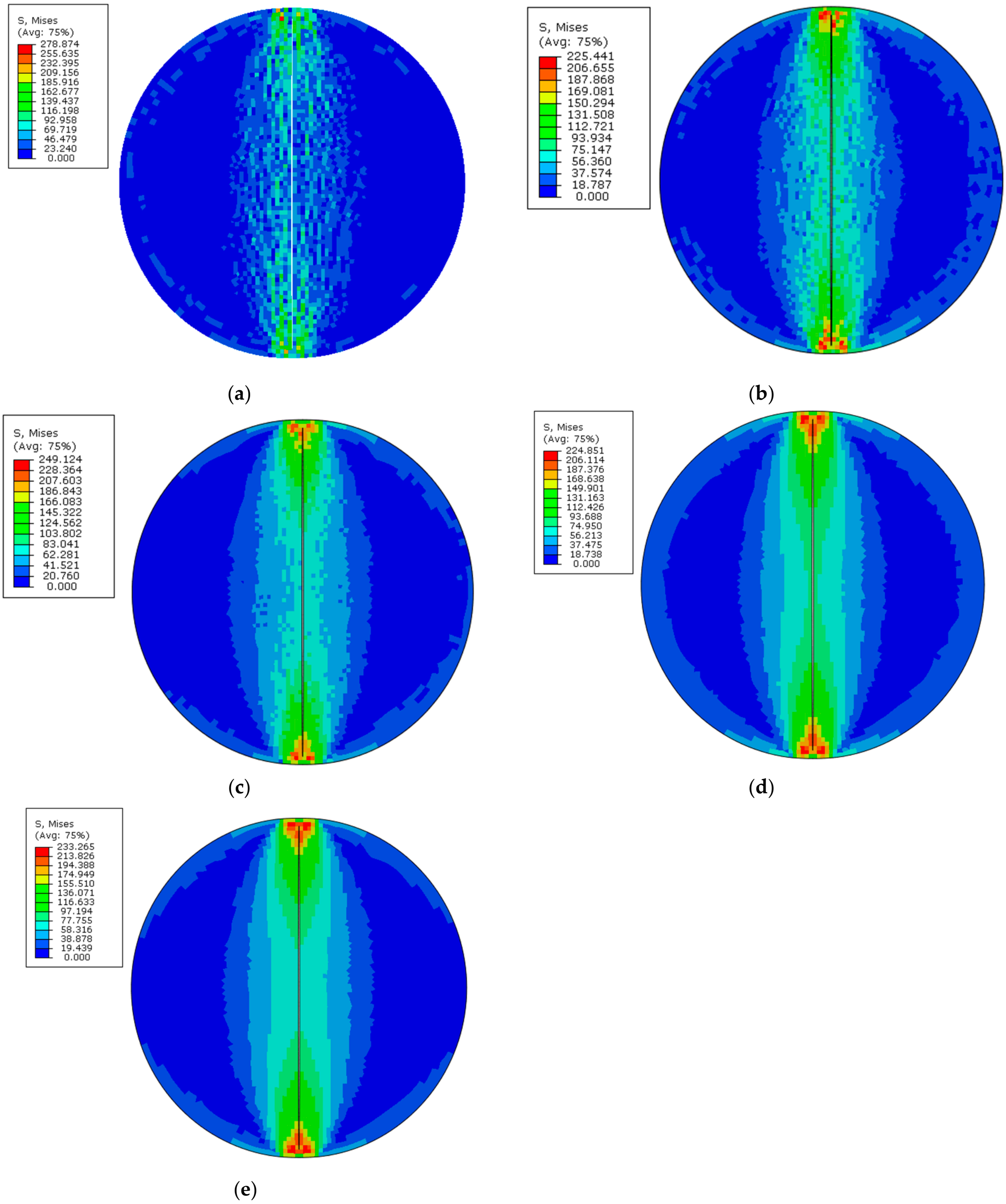

Figure 13. Numerical simulation of Brazilian splitting for heterogeneous model. (**a**) m = 1.5; (**b**) m = 5; (**c**) m = 10; (**d**) m = 100; (**e**) m = 1000.

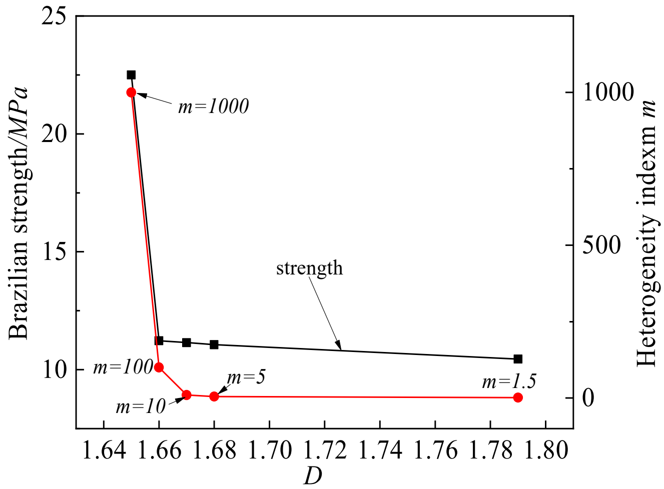

Figure 14. Relationship of D and Brazilian strength and m.

The stress–displacement curves of the rock specimens with different homogeneities are shown in Figure 15. The rock specimens with $1.5 \leq m \leq 100$ under Brazilian splitting load all underwent the three stages of linear elasticity, yielding, and post-peak. The difference among all the stress–displacement curves is that their yielding phase becomes shorter with the increase in homogeneity. When $5 \leq m \leq 100$, the stress–displacement curves almost coincided. When m is greater than 1000, the yield phase is almost unrecognizable, and the rock sample breaks directly after the linear elastic phase. Regardless of the homogeneity of the rock, brittle damage is evident under Brazilian splitting loads.

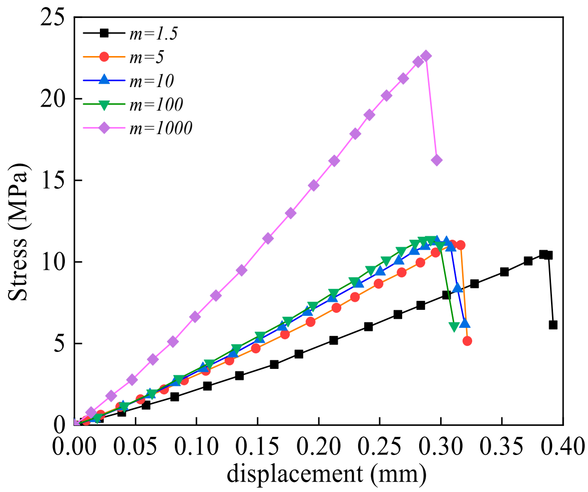

Figure 15. Stress–displacement curves in different homogeneity cases.

4. Discussion

4.1. Ubiquitiformal Complexity

In ubiquitiform theory, for a given ubiquitiform, a fractal that corresponds to its iterative process generally exists. The complexity of the ubiquitiform is defined as the dimension of the adjoint fractal [43]. The ubiquitiformal complexity can be used to characterize the bending and roughness of the curve. The greater the ubiquitiformal complexity is, the rougher the curve will be, and vice versa [21]. The box-counting method is now commonly used to calculate the ubiquitiformal complexity [19,35]. This method relies on digital analysis and is calculated using a box-dimensional algorithm written in MATLAB, which is the method used in this paper.

The concept of ubiquitiform was applied to the field of rock mechanics to characterize fracture surface roughness and pore structure. In recent years, Zhang [23] has simulated the extension of heterogeneous model cracks under different Weibull homogeneity distributions. The more homogeneous the material is, the less complex its crack path is. The basic idea that the heterogeneous characteristics of the material can lead to ubiquitiform cracks of the specimen was verified. Li et al. [22] used ABAQUS numerical simulation software to study the ubiquitiform crack extension in heterogeneous quasi-brittle materials by numerical simulation. The ubiquitiformal complexity of the section configuration is given using the box-counting dimension calculation, and the correlation between the fracture energy and complexity is determined. Based on ubiquitiform theory and fracture mechanics, Dong [44] proposed a calculation method for material fracture surface complexity and tested its validity computationally.

In this paper, by comparing the ubiquitiformal complexity of slate and granite, we found that the ubiquitiformal complexity of slate ranges from 1.54 to 1.60, and that of granite ranges from 1.58 to 1.62. The complexity is related to the properties of the material. For the same type of rock, the complexity size does not basically vary much under the same loading conditions. However, due to the difference in rock properties, the ubiquitiformal complexity of granite is generally larger than that of slate. In Section 3.4, two numerical models are established in this paper. Analysis suggests that the granite ubiquitiformal complexity under the ideal homogeneous model is 1.65, and the relative error between the average ubiquitiformal complexity of granite obtained from the experiment is 0.03%. The ubiquitiformal complexity of the heterogeneous model at different homogeneity levels ranges from 1.65 to 1.79. In the comparison of the ubiquitiformal complexity of the two models, we obtain that the ubiquitiformal complexity of the rock is higher for a homogeneity m of 1.5. The ubiquitiformal complexity with m greater than five is closer to that of the ideal homogeneous model. Thus, this finding shows that the extension path of the ubiquitiformal crack gradually tends to be smooth when m is larger than five.

4.2. Fracture Energy

In classical fracture mechanics, fracture energy is an important parameter in characterizing the fracture properties of a material. It is defined as the amount of energy required to produce a new cracked surface per unit area and is of great importance in engineering safety design [45,46]. Currently, fracture energy can be calculated using three methods, namely, the traditional fracture energy which only considers the cross-sectional area of the smooth section, the fracture energy obtained from the fracture toughness, and the ubiquitiformal fracture energy that considers the ubiquitiform characteristics of the material section. The inconsistency between the fracture energy obtained from fracture toughness and the traditional fracture energy has long concerned scholars. The usual assumption of presumed linear elasticity does not provide a good approximation of the physical properties of real materials, and therefore, ubiquitiformal fracture energy is proposed. The establishment of ubiquitiform theory can solve the difficulties of requiring infinite energy for material damage and the fact that reformation fracture energy is no longer suitable as a material property parameter [23].

The calculation of the ubiquitiformal fracture energy is very simple, as long as the traditional fracture energy and the lower bound to scale invariance are determined. The ubiquitiformal fracture energy can be obtained according to Equation (5). An important issue that needs to be considered in solving the ubiquitiformal fracture energy is the influence of the lower bound to scale invariance on the calculation results. The lower bound to scale invariance affects the integer dimensional measurement of the ubiquitiform directly. Therefore, discussing the lower bound to scale invariance further is necessary to avoid the error caused by the practical application. This value is currently believed to be a material constant, which is determined by the microstructure of the studied object. However, providing a specific method for determining this value, which is usually taken as the fundamental particle size of the studied object, is not yet possible, and this method is usually imprecise. Li et al. [47] proposed the use of the equation between the tensile strength and the lower bound to scale invariance to determine the value, and this method is only suitable for concrete materials. Cao et al. [48] relied on digital image analysis and the calculation of the box dimension algorithm based on MATLAB. The relationship curve between the measurement and the scale invariance in double logarithmic coordinates is obtained and fitted to it. The linear segment with a better fitting effect is taken as the self-similar region of the ubiquitiform to determine the lower bound to scale invariance. This approach is relatively rough because of the image resolution. Therefore, this paper summarizes the previous experience and assumes that the ubiquitiformal fracture energy tends to be constant, and the ubiquitiformal fracture energy is calculated according to different lower bound to scale invariances. When the mean square deviation coefficient of the ubiquitiformal fracture energy is minimum, the lower bound to scale invariance is chosen as the desired result. This method is implemented with the help of MATLAB. By calculation, the lower bound to scale invariance for slate and granite is 1.4 μm and 4.7μm, respectively. From the analysis of the mineral composition, the particle size of granite is generally 1–5 mm, and the particle size of the slate is 0.0039–0.0625 mm, which causes the bound to scale invariance of granite to be lower than that of slate.

The fracture energy calculated in this paper considers the ubiquitiformal complexity in the thickness direction and is the fracture energy on a two-dimensional measure. The three fracture energies are analyzed in Section 2.3. The calculation result of the ubiquitiformal fracture energy G_{uf} is concluded to be very close to the critical strain energy release rate G_c obtained from the fracture toughness relationship while differing significantly from the traditional fracture energy G. This conclusion is also consistent with those obtained from previous experiments [39]. In addition, the ubiquitiformal fracture energy of the same type of rock is relatively close, indicating that the cracks in the fracture of rock materials have a good consistency. The ubiquitiformal fracture energy is more consistent with the assumption of the linear elastic fracture of brittle materials than the fracture energy measured under the assumption of a smooth fracture surface. In a fundamental sense, traditional fracture energy only considers the cross-sectional area of a smooth section and represents only the average energy release rate of the section. Meanwhile, the critical strain energy release rate considers the critical crack tip energy release rate and describes the local fracture properties of the material. The real crack surface is actually rough. Thus, considering its real crack extension path is necessary. While real crack extension leads to increasingly complex stress singularities at the crack tip, the ubiquitiformal fracture energy is calculated for the ubiquitiformal cross-sectional area alone, thereby providing similar results to the critical strain energy release rate. This finding verifies that the cross-sectional area is more important than the crack tip stress singularity. In addition, in this paper, the mean values and mean squared deviations of the three fracture energies for slate and granite were obtained, and the mean squared deviations of the ubiquitiformal fracture energy were the smallest among the other fracture energies. The reliability of the ubiquitiformal fracture energy was further verified.

4.3. Heterogeneity Effect

In general, the study of mechanical properties and damage processes of rocks is based on the assumption that rocks are homogeneous materials. However, rocks are heterogeneous materials at the microscopic scale, and the spatial distribution of their physical and mechanical properties is discontinuous. Heterogeneity has a significant influence on the mechanics of rock. To analyze the relationship between the Brazilian splitting strength and homogeneity m, the elastic modulus of the mesoscopic element of the constituent material is assumed to satisfy the Weibull distribution. The Weibull distribution parameters m are set to 1.5, 5, 10, 100, and 1000. In Section 3.4.2, the curve between the Brazilian splitting strength and the homogeneity, where the homogeneity m describes the degree of homogeneity of the micromechanical properties of the rock material, is plotted.

When homogeneity is less than 1.5, heterogeneity has a greater influence on the Brazilian splitting strength, and the heterogeneity of the rock becomes evident. At this time, the yielding phase of the stress–displacement curve is the longest. However, when the homogeneity is $5 \leq m \leq 100$, the effect on the Brazilian splitting strength is much less, the Brazilian splitting strength tends to the average strength, and the stress–displacement curves almost coincide. This phenomenon can be explained by the fact that as the homogeneity decreases, the discreteness of the material parameters increases and some units fail at low stresses, thereby reducing the strength of the rock specimens. As homogeneity increases, the mechanical parameters of the units become more concentrated, the number of units with lower mechanical parameters decreases, the overall strength of the crack tip region increases, and the rock exhibits brittle failure. When m is greater than 1000, the yield phase is almost unrecognizable, and the rock sample breaks directly after the linear elastic phase. Heterogeneity and size effects influence the difference in the Brazilian splitting strength of rocks by different test homogeneity m [49–51]. In this paper, only the effect of heterogeneous properties is considered. Therefore, investigating the size effect in the future is necessary.

5. Conclusions

In this paper, the type I crack extension problem is investigated on the basis of ubiquitiform theory. First, the complexity of the fractured section of slate and granite after Brazilian splitting was calculated. Second, the expression of the ubiquitiformal fracture energy during crack extension is studied theoretically, and the fracture energy is compared under three calculation methods. Finally, the Brazilian splitting test was simulated using finite element software. The homogeneous and heterogeneous models of granite were established and compared with the experimental results to verify the rationality of the models. In addition, the relationship between the ubiquitiformal complexity and homogeneity and Brazilian splitting strength under the heterogeneous model is discussed. The conclusions are summarized as follows:

The ubiquitiformal complexity of slate ranges from 1.54 to 1.60, and that of granite ranges from 1.58 to 1.62. However, the ubiquitiformal complexity of granite is generally larger than that of slate because of the difference in rock properties.

The calculation result of the ubiquitiformal fracture energy G_{uf} is very close to the critical strain energy release rate G_c obtained from the fracture toughness relationship while differing significantly from the traditional fracture energy G. Therefore, the ubiquitiformal fracture energy is more consistent with the assumption of the linear elastic fracture of brittle materials than the fracture energy measured under the assumption of the smooth fracture surface.

The numerical simulation results of the ideal homogeneous model are basically consistent with the experimental results. Under compressive loading, stress concentration occurs at the crack tip, and stress is symmetrical about the crack plane. The damage begins when the stress at the crack tip reaches its maximum and the crack develops along the central loading line until the material fails completely.

When the homogeneity of the heterogeneous model is $m = 1.5$, the distribution of the stress concentration area is neither regular nor clear because of the discrete elastic modulus of the unit and the significant difference in stresses in adjacent units. As the homogeneity increases (1.5–5), the discreteness of unit strength and elastic modulus decreases, and the overall strength of the crack tip region increases and gradually converges to a constant. When homogeneity is 1000, the mechanical properties improve rapidly. In addition, the Brazilian splitting strength decreases as the ubiquitiformal complexity increases. The heterogeneity of the rocks is evident at an m of 1.5, and when $5 < m < 100$, the variation of the ubiquitiformal complexity of the rock is small, which belongs to low homogeneity. When m is 1000, the effect of the heterogeneous properties of the material is eliminated.

Author Contributions: Conceptualization, writing—original draft, writing—review and editing, investigation, formal analysis, supervision, project administration funding acquisition, B.Y.; investigation, X.C., T.H., P.L. and J.S. All authors have read and agreed to the published version of the manuscript.

Funding: This research is funded by the National Natural Science Foundation of China (Nos. 11872300, 11572244). It also was supported by the Natural Science Foundation of Shaanxi Province, China (No. 2021JQ-463, 2021JZ-47), and the Youth Innovation Team of Shaanxi Universities.

Data Availability Statement: The data that support the findings of this study are available from the corresponding author upon reasonable request.

Conflicts of Interest: The authors declare no conflict of interest.

References

1. Mandelbrot, B.B.; Passoja, D.E.; Paullay, A.J. Fractal character of fracture surfaces of metals. *Nature* **1984**, *308*, 721–722. [CrossRef]
2. Panigrahy, C.; Seal, A.; Mahato, N.K. Quantitative texture measurement of gray-scale images: Fractal dimension using an improved differential box counting method. *Measurement* **2019**, *147*, 106859. [CrossRef]
3. Meng, T.; Xie, J.; Li, X.M.; Ma, J.W.; Yue, Y. Experimental study on the evolutional trend of pore structures and fractal dimension of low-rank coal rich clay subjected to a coupled thermo-hydro-mechanical-chemical environment. *Energy* **2020**, *203*, 117838.
4. Yang, A.; Li, S.; Lin, H.; Jin, D. Edge extraction of mineralogical phase based on fractal theory. *Chaos Solitons Fractals* **2018**, *117*, 215–221.
5. Zhang, K.; Liu, X.; Liu, W.; Zhang, S. Influence of weak inclusions on the fracturing and fractal behavior of a jointed rock mass containing an opening: Experimental and numerical studies. *Comput. Geotech.* **2021**, *132*, 104011. [CrossRef]
6. Cai, W.; Cen, G.; Wang, H. Fracture Surface Fractal Characteristics of Alkali-Slag Concrete under Freeze-Thaw Cycles. *Adv. Mater. Sci. Eng.* **2017**, *2017*, 1689893. [CrossRef]
7. Gu, F.; Zhang, J.; Chen, Y. Fractal dimension of scattering equivalent section of aerosol and its calibration mechanism. *Chin. Opt. Lett.* **2009**, *7*, 857–860.
8. Hao, L.; Tang, J.; Wang, Q.; Tao, H.; Ma, X.; Ma, D.; Ji, H. Fractal characteristics of tight sandstone reservoirs: A case from the Upper Triassic Yanchang Formation, Ordos Basin, China. *J. Pet. Sci. Eng.* **2017**, *158*, 243–252. [CrossRef]
9. Dang, N.; Tao, J.; Zeng, Q.; Zhao, W. May the Piezoresistivity of GNP-Modified Cement Mortar Be Related to Its Fractal Structure? *Fractal Fract.* **2021**, *5*, 148. [CrossRef]
10. He, W.; Hayatdavoudi, A.; Shi, H.; Sawant, K.; Huang, P. A Preliminary Fractal Interpretation of Effects of Grain Size and Grain Shape on Rock Strength. *Rock Mech. Rock Eng.* **2019**, *52*, 1745–1765. [CrossRef]
11. Niu, D.; Huang, D.; Zheng, H.; Su, L.; Fu, Q.; Luo, D. Experimental Study on Mechanical Properties and Fractal Dimension of Pore Structure of Basalt–Polypropylene Fiber-Reinforced Concrete. *Appl. Sci.* **2019**, *9*, 1602. [CrossRef]
12. Yang, L.-L.; Xu, W.-Y.; Meng, Q.-X.; Wang, R.-B. Investigation on jointed rock strength based on fractal theory. *J. Cent. South Univ.* **2017**, *24*, 1619–1626. [CrossRef]
13. Xiao, J.; Long, X.; Li, L.; Jiang, H.; Zhang, Y.; Qu, W. Study on the Influence of Three Factors on Mass Loss and Surface Fractal Dimension of Concrete in Sulfuric Acid Environments. *Fractal Fract.* **2021**, *5*, 146. [CrossRef]
14. Gao, Y.; Gao, F.; Yeung, M.-C.R. A Fractal and Numerical Simulation Coupled Study of Fracture Network during Coal Mining Excavation. *J. Appl. Math.* **2014**, *2014*, 158194. [CrossRef]
15. Giri, A.; Tarafdar, S.; Gouze, P.; Dutta, T. Fractal pore structure of sedimentary rocks: Simulation in 2-d using a relaxed bidisperse ballistic deposition model. *J. Appl. Geophys.* **2012**, *87*, 40–45. [CrossRef]
16. Wu, D.; Hu, Y.; Fan, X. Visual simulation for granular rocks crush in virtual environment based on fractal geometry. *Simul. Model. Pract. Theory* **2009**, *17*, 1254–1266. [CrossRef]
17. Xiao, J.; Xu, Z.; Murong, Y.; Wang, L.; Lei, B.; Chu, L.; Jiang, H.; Qu, W. Effect of Chemical Composition of Fine Aggregate on the Frictional Behavior of Concrete–Soil Interface under Sulfuric Acid Environment. *Fractal Fract.* **2021**, *6*, 22. [CrossRef]
18. Wang, L.; Lu, X.; Liu, L.; Xiao, J.; Zhang, G.; Guo, F.; Li, L. Influence of MgO on the Hydration and Shrinkage Behavior of Low Heat Portland Cement-Based Materials via Pore Structural and Fractal Analysis. *Fractal Fract.* **2022**, *6*, 40. [CrossRef]
19. Ou, Z.-C.; Li, G.-Y.; Duan, Z.-P.; Huang, F.-L. Ubiquitiform in Applied Mechanics. *J. Theor. Appl. Mech.* **2014**, *52*, 37–46.
20. Li, G.-Y.; Ou, Z.-C.; Xie, R.; Duan, Z.-P.; Huang, F.-L. A Ubiquitiformal One-Dimensional Steady-State Conduction Model for a Cellular Material Rod. *Int. J. Thermophys.* **2016**, *37*, 41. [CrossRef]
21. Ou, Z.-C.; Yang, M.; Li, G.-Y.; Duan, Z.-P.; Huang, F.-L. Ubiquitiformal fracture energy. *J. Theor. Appl. Mech.* **2017**, *55*, 1101–1108. [CrossRef]
22. Li, J.Y.; Gao, W.X.; Song, X.L. Numerical simulation on the extension of a ubiquitiformal crack of rock materials under dynamic loading. *Vib. Shock* **2018**, *37*, 88–91+103.
23. Zhang, N. Characterization of Crack Propagation Fracture Parameters Based on the Ubiquitiform Theory. Master's Thesis, Xi'an University of Technology, Xi'an, China, 2019.
24. You, M.-Q.; Zou, Y.-F. Discussion on heterogeneity of rock material and size effect on specimen strength. *Chin. J. Rock Mech. Eng.* **2000**, *19*, 391–395.
25. Li, M.; Guo, P.; Stolle, D.F.; Liang, L.; Shi, Y. Modeling hydraulic fracture in heterogeneous rock materials using permeability-based hydraulic fracture model. *Undergr. Space* **2020**, *5*, 167–183. [CrossRef]
26. Li, S.-C.; Li, G.-Y. Effect of heterogeneity on mechanical and acoustic emission characteristics of rock specimen. *J. Cent. South Univ. Technol.* **2010**, *17*, 1119–1124. [CrossRef]

27. Wang, J.-T.; Zuo, J.-P. Numerical simulation on effect of heterogeneity on mode I fracture characteristics of rock. *J. Cent. South Univ.* **2020**, *27*, 3063–3077. [CrossRef]
28. Fu, B.; Li, Y.; Tang, C.; Lin, Z. Failure of Rock Slope with Heterogeneous Locked Patches: Insights from Numerical Modelling. *Appl. Sci.* **2021**, *11*, 8585. [CrossRef]
29. Xu, Y.; Yao, W.; Xia, K. Numerical study on tensile failures of heterogeneous rocks. *J. Rock Mech. Geotech. Eng.* **2020**, *12*, 50–58. [CrossRef]
30. Lan, H.; Martin, C.D.; Hu, B. Effect of heterogeneity of brittle rock on micromechanical extensile behavior during compression loading. *J. Geophys. Res. Solid Earth* **2010**, *115*, B01202. [CrossRef]
31. Liao, Z.; Zhu, J.; Tang, C. Numerical investigation of rock tensile strength determined by direct tension, Brazilian and three-point bending tests. *Int. J. Rock Mech. Min. Sci.* **2019**, *115*, 21–32. [CrossRef]
32. Ju, Y.; Ou, Z.; Duan, Z.; Huang, F. The Ubiquitiformal Characterization of the Mesostructures of Polymer-Bonded Explosives. *Materials* **2019**, *12*, 3763. [CrossRef] [PubMed]
33. Yang, M.; Ou, Z.-C.; Duan, Z.-P.; Huang, F.-L. Research on one-dimensional ubiquitiformal constitutive relations for a bimaterial bar. *J. Theor. Appl. Mech.* **2019**, *57*, 291–301. [CrossRef]
34. He, M.; Li, N.; Zhu, C.; Chen, Y.; Wu, H. Experimental investigation and damage modeling of salt rock subjected to fatigue loading. *Int. J. Rock Mech. Min. Sci.* **2019**, *114*, 17–23. [CrossRef]
35. Ou, Z.-C.; Li, G.-Y.; Duan, Z.-P.; Huang, F.-L. A stereological ubiquitiformal softening model for concrete. *J. Theor. Appl. Mech.* **2019**, *57*, 27–35. [CrossRef]
36. Shang, S.; Cao, X.; Liu, Z.; Shi, J. Analysis of Normal Elastic Contact Stiffness of Rough Surfaces Based on Ubiquitiform Theory. *J. Tribol.* **2019**, *141*, 111401. [CrossRef]
37. Wang, Q.Z.; Wu, L.Z. Determination of elastic modulus, tensile strength and fracture toughness of brittle rock with platform Brazilian disc specimens–Part II: Test results. *Chin. J. Rock Mech. Eng.* **2004**, *2*, 199–204.
38. Grodner, M.W.; Clarke, S.M.; Burley, S.D.; Leslie, A.G.; Haslam, R. Combining topology and fractal dimension of fracture networks to characterise structural domains in thrusted limestones. *J. Struct. Geol.* **2021**, *153*, 104468. [CrossRef]
39. Zhang, H.; Wei, D.-M. Estimation of fracture toughness, driving force, and fracture energy for fractal cracks using the method of imaginary smooth crack. *Eng. Fract. Mech.* **2010**, *77*, 621–630. [CrossRef]
40. Emami, S.-M.; Mousavi, S.-F.; Hosseini, K.; Fouladfar, H.; Mohammadian, M. Comparison of different turbulence models in predicting cohesive fluid mud gravity current propagation. *Int. J. Sediment Res.* **2020**, *35*, 504–515. [CrossRef]
41. Qiu, H.; Zhu, Z.; Wang, M.; Wang, F.; Luo, C.; Wan, D. Study of the failure properties and tensile strength of rock-mortar interface transition zone using bi-material Brazilian discs. *Constr. Build. Mater.* **2020**, *236*, 117551. [CrossRef]
42. Saksala, T.; Hokka, M.; Kuokkala, V.-T.; Mäkinen, J. Numerical modeling and experimentation of dynamic Brazilian disc test on Kuru granite. *Int. J. Rock Mech. Min. Sci.* **2013**, *59*, 128–138. [CrossRef]
43. Li, J.-Y.; Ou, Z.-C.; Tong, Y.; Duan, Z.-P.; Huang, F.-L. A statistical model for ubiquitiformal crack extension in quasi-brittle materials. *Acta Mech.* **2017**, *228*, 2725–2732. [CrossRef]
44. Dong, Y.X. Study on the Ubiquitiformal Fracture Characteristics of Brittle Metals. Master's Thesis, Xi'an University of Technology, Xi'an, China, 2019.
45. Muralidhara, S.; Prasad, B.R.; Singh, R. Size independent fracture energy from fracture energy release rate in plain concrete beams. *Eng. Fract. Mech.* **2013**, *98*, 284–295. [CrossRef]
46. Yu, K.; Yu, J.; Lu, Z. Average Fracture Energy for Crack Propagation in Postfire Concrete. *Adv. Mater. Sci. Eng.* **2013**, *2013*, 143208. [CrossRef]
47. Li, G.Y.; Ou, Z.C.; Yu, B.; Huang, F.L. Fractal cohesion model of concrete under tensile load. *Chin. J. Solid Mech.* **2012**, *33*, 251–257.
48. Cao, H.L. Based on the Ubiquitiform Theory Method to the Contact Stiffness of Mechanical Joint Surface is Studied. Master's Thesis, Xi'an University of Technology, Xi'an, China, 2018.
49. Alam, S.Y.; Zhu, R.; Loukili, A. A new way to analyse the size effect in quasi-brittle materials by scaling the heterogeneity size. *Eng. Fract. Mech.* **2020**, *225*, 106864. [CrossRef]
50. Del Giudice, M. Addendum to: Heterogeneity Coefficients for Mahalanobis' D as a Multivariate Effect Size. *Multivar. Behav. Res.* **2018**, *53*, 571–573. [CrossRef] [PubMed]
51. Olsson-Collentine, A.; Wicherts, J.M.; van Assen, M.A.L.M. Heterogeneity in direct replications in psychology and its association with effect size. *Psychol. Bull.* **2020**, *146*, 922–940. [CrossRef]